

## ***CYP2J19* mediates carotenoid colour introgression across a natural avian hybrid zone**

Alexander N. G. Kirschel<sup>1,\*</sup>, Emmanuel C. Nwankwo<sup>1</sup>, Daniel Pierce<sup>2</sup>, Michaella Moysi<sup>1</sup>,  
Bridget O. Ogolowa<sup>1</sup>, Ara Monadjem<sup>3,4</sup> and Alan Brelsford<sup>2</sup>

<sup>1</sup>Department of Biological Sciences, University of Cyprus, PO Box 20537, Nicosia 1678, Cyprus

<sup>2</sup>Evolution, Ecology, and Organismal Biology Department, University of California Riverside, Riverside, CA, 92521, USA

<sup>3</sup>Department of Biological Sciences, University of Eswatini, Private Bag 4, Kwaluseni, Eswatini

<sup>4</sup>Mammal Research Institute, Department of Zoology & Entomology, University of Pretoria, Private Bag 20, Hatfield, Pretoria 0028, South Africa

\*Correspondence

Alexander Kirschel, Department of Biological Sciences, University of Cyprus, PO Box 20537, Nicosia 1678, Cyprus  
Email: kirschel@ucy.ac.cy

Running head: Genes for red and yellow feathers across a hybrid zone

### **Abstract**

It has long been of interest to identify the phenotypic traits that mediate reproductive isolation between related species, and more recently, the genes that underpin them. Much work has focused on identifying genes associated with animal colour, with the candidate gene *CYP2J19* identified in laboratory studies as the ketolase converting yellow dietary carotenoids to red ketocarotenoids in birds with red pigments. However, evidence that *CYP2J19* explains variation between red and yellow feather coloration in wild populations of birds is lacking. Hybrid zones provide the opportunity to identify genes associated with specific traits. Here we investigate

genomic regions associated with colour in red-fronted and yellow-fronted tinkerbirds across a hybrid zone in southern Africa. We sampled 85 individuals, measuring spectral reflectance of forecrown feathers and scoring colours from photographs, while testing for carotenoid presence with Raman spectroscopy. We performed a genome-wide association study to identify associations with carotenoid-based coloration, using double-digest RAD sequencing aligned to a short-read whole genome of a *Pogoniulus* tinkerbird. Admixture mapping using 104,933 single nucleotide polymorphisms (SNPs) identified a region of chromosome 8 that includes *CYP2J19* as the only locus with more than two SNPs significantly associated with both crown hue and crown score, while Raman spectra provided evidence of ketocarotenoids in red feathers. Asymmetric backcrossing in the hybrid zone suggests that yellow-fronted females mate more often with red-fronted males than vice versa. Female red-fronted tinkerbirds mating assortatively with red-crowned males is consistent with the hypothesis that converted carotenoids are an honest signal of quality.

**Keywords:** asymmetric backcrossing, introgressive hybridization, *Pogoniulus* tinkerbirds, plumage coloration, sexual selection, speciation.

## 1 INTRODUCTION

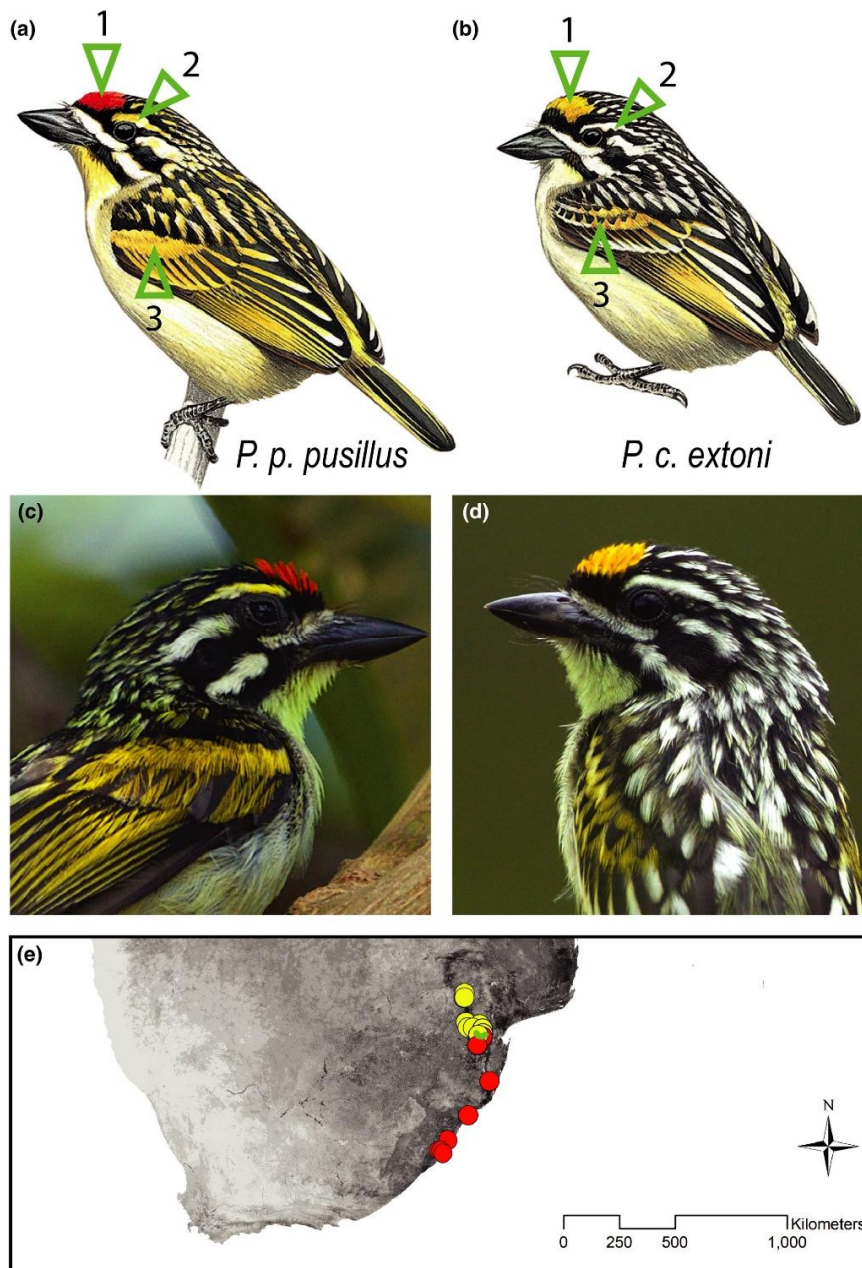
For centuries, species have been classified based on their physical appearance. Early naturalists differentiated between species based on functional traits such as jaw and limb shape, and beak size, or otherwise on traits that function in social selection, such as fur pattern and plumage coloration (Birkhead, 2008; Leroi, 2014). Such phenotypic characters, representing clear visual differences to the human eye, have been thought to aid the species themselves in

recognizing their own kind and finding potential mates. It has long been of interest to identify which traits mediate reproductive isolation between related species (Mayr, 1942), and more recently, which genes underpin those traits: in other words, the genes that mediate speciation (Nosil & Schluter, 2011). Hybrid zones between related species provide an unparalleled opportunity to identify genes associated with phenotypic characters (Brelsford et al., 2017; Delmore et al., 2016), including those that play an important role in mate choice and species recognition (Harrison & Larson, 2016). In some such cases, it is just a small set of genes that maintain phenotypic differences between hybridizing taxa, especially those functioning in coloration and pattern differences (Poelstra et al., 2014; Toews et al., 2016). Additionally, evidence is mounting that the extent of divergence in plumage coloration between populations affects assortative mating (Billerman et al., 2019; Haas et al., 2009; Hill & McGraw, 2004; Saetre et al., 1997; Scordato et al., 2017).

Genes involved in coloration and patterning pathways have received considerable attention (Hoekstra, 2006; Mundy, 2005), with a number of recent studies identifying genes associated with the melanin pigmentation pathway by studying variation across hybrid zones (e.g., Campagna et al., 2017; Delmore et al., 2016; Toews et al., 2016; Walsh et al., 2016). Carotenoid-based coloration, incorporating the reds, oranges and yellows, has received far less attention (Toews et al., 2017), because carotenoid uptake is dependent on diet (McGraw, 2006), meaning that identifying the genes involved in carotenoid processing is especially challenging (Campagna et al., 2017). Nevertheless, much progress has been made recently, with the scavenger receptor B1 (*SCARB1*) identified as a mediator of carotenoid-colour expression in birds (Toomey et al., 2017), *RALY* has been identified as playing a role in the relative intensity of carotenoid versus melanin pigmentation (Nadeau et al., 2008; Wang et al., 2019), while a region

of the Z chromosome has been identified as a potential regulatory region for *follistatin* and is associated with sex-linked red colour polymorphism in Gouldian finch *Erithrura gouldiae* (Kim et al., 2019). In addition, the carotenoid cleaving enzyme  $\beta$ -carotene oxygenase 2 (*BCO2*) has been shown to function in red bare part coloration and even sexual dichromatism in laboratory crosses of yellow canaries and red siskins known as “mosaic” canaries (Gazda, et al., 2020; Gazda, et al., 2020). Previous work has also identified candidate genes to explain differences between red and yellow feather coloration through another laboratory cross of yellow canaries with red siskins known as “red factor” canaries (Lopes et al., 2016) and between red- and orange-billed individuals of zebra finches (Mundy et al., 2016). Both studies specifically identified the gene *CYP2J19* as the one that encodes the ketolases that catalyse the conversion of yellow dietary carotenoids to red C4-ketocarotenoids. Both studies were focused on laboratory-based crosses involving artificially selected forms of species developed to express certain traits (“red factor” canaries and “yellowbeak” zebra finches respectively). A field-based study in long-tailed finch *Poephila acuticauda* provided further support for the role of *CYP2J19* in carotenoid-based bill colour across a natural hybrid zone (Hooper et al., 2019), while *CYP2J19* gene expression has also been associated with red coloration in weaverbirds (Twyman et al., 2018). An in silico approach producing a molecular model of *CYP2J19* also suggested its role in ketolation in house finches, and that its efficiency was associated with mitochondrial function (Hill et al., 2019). However, evidence of its role in explaining variation between red and yellow feather coloration in wild populations of birds is lacking. Indeed, there are potentially other pathways, with a number of examples of species with red or orange feather colour produced without the presence of ketocarotenoids (Andersson et al., 2007; Brush, 1970; Twyman, et al., 2018).

Red-fronted (*Pogoniulus pusillus*, Dumont, 1816) and yellow-fronted (*P. chrysoconus*, Temminck, 1832) tinkerbirds provide such an opportunity to investigate the genes involved in carotenoid processing because they hybridize extensively at a contact zone in southern Africa (Nwankwo et al., 2019). They differ phenotypically most noticeably in their forecrown coloration; hence their vernacular names (Figure 1). Their other plumage differences are also in carotenoid-based colours, but those are more subtle differences, to the human eye at least, between shades of yellow and white that characterize the colour of their underparts, rump, wing bar and supercilium (Hockey et al., 2005). The extent to which these differences might play a role in mate choice is not yet known. The two species have been shown to hybridize extensively with asymmetric introgression of red forecrown plumage into the *P. chrysoconus* genomic background, in spite of phylogenetic analysis on mitochondrial DNA (mtDNA) revealing the two species have been diverging for over 4 million years (Nwankwo et al., 2019). Despite the deep divergence between the species, the extent of introgression indicates that hybrids are viable and fertile, although some reduced hybrid fitness might maintain a tension zone preventing the two species of collapsing into one, as has been found in ravens (Kearns et al., 2018). Thus, if at least one of the two species continues to differentiate between the two phenotypes and mates only with individuals of its own phenotype, the plumage trait and the genes underlying it may play an important role in maintaining species divergence.



**Figure 1.** Forecrown plumage (1) coloration was scored in: (a) *Pogoniulus pusillus pusillus* and (b) *Pogoniulus chrysoconus extoni*. We also scored: (2) supercilium and (3) wing bar extent of yellow over black, from photographs, as shown of (c) *P. p. pusillus* and (d) *P. c. extoni* from allopatric populations. Samples, photographs scored and forecrown feathers were obtained from individuals phenotypically red-fronted (red circles) and yellow-fronted (yellow circles) across the contact zone (green line) in southern Africa (e). Illustrations courtesy of del Hoyo et al. (2020)

Here we investigate the genomic regions associated with the red and yellow feathers in red-fronted and yellow-fronted tinkerbirds that could play an important role in reproductive isolation. Our study is based on samples from 85 individuals previously collected across the hybrid zone in southern Africa, including forecrown feathers used in spectrophotometric analysis (Nwankwo et al., 2019). A subset of forecrown feathers was used to identify the presence of carotenoids and differences between red and yellow feathers using Raman spectroscopy (Thomas et al., 2014; Veronelli et al., 1995). We performed a genome-wide association study (GWAS) to identify single nucleotide polymorphisms (SNPs) associated with plumage coloration. The study included assembly of a short-read genome of an individual *P. pusillus* and double-digest restriction association DNA sequencing (ddRAD). Our aim was to identify the genes associated with carotenoid plumage coloration across a natural contact zone, and specifically which regions of the genome explain differences between red and yellow plumage. We further tested whether those genes, or SNPs at other loci, might be associated with the shade of yellow to white or extent of yellow versus black plumage in other feather patches. We then compared alleles at loci associated with forecrown colour with the hybrid index across autosomes and the Z chromosome, and interspecific heterozygosity of individuals, to elucidate the patterns of interbreeding across genotypes that explain asymmetric introgression between species that have been diverging for over 4 million years (Nwankwo et al., 2019).

## **2 MATERIALS AND METHODS**

### ***2.1 Study species and sample collection***

*Pogoniulus* tinkerbirds are African barbets (Lybiidae) that although omnivorous, feed primarily on fruit, especially mistletoe (Dowsett-Lemaire, 1988; Godschalk, 1985). Species in the genus

differ subtly in plumage characters despite millions of years of divergence in mtDNA between currently recognized sister species (Kirschel et al., 2009, 2018; Nwankwo et al., 2018, 2019). *Pogoniulus pusillus pusillus* (hereafter *pusillus*) and *P. chrysoconus extoni* (Layard, 1871) (hereafter *extoni*) are the subspecies of red-fronted and yellow-fronted tinkerbird, respectively, that meet at a contact zone in southern Africa (Monadjem et al., 1994). The two species overlap in diet, with a preference in particular for *Tapinanthus* spp. mistletoe fruits (Hockey et al., 2005). They occur together in broad-leaved woodland in the contact zone, with *extoni* occupying Miombo woodland and *pusillus* dry coastal and evergreen forest in allopatry (Hockey et al., 2005). They differ in plumage characters beyond the forecrown colour in the yellower supercilium and dorsal streaking in *pusillus*—whiter in *extoni*, the deeper amber and greater percentage of carotenoid pigment over melanin pigment on the wing coverts in *pusillus*—and paler yellow with more black in *extoni* (Figure 1). The two species also differ more subtly in underpart coloration, such as in throat and breast colour (Hockey et al., 2005).

Fieldwork was performed at 16 sites across the contact zone where subspecies *extoni* and *pusillus* meet in southern Africa and in more distant allopatry. Fieldwork took place in Tanzania in June–September 2013, and in South Africa and Eswatini in March and December 2015, and January–February 2017. Methods used to obtain DNA and feather samples have been previously described (Nwankwo et al., 2019). Briefly, 85 birds were captured in mist-nets, of which 49 were from the contact zone. Blood samples were obtained via venepuncture of the brachial vein, and crown feathers were plucked and placed in envelopes for spectral reflectance analysis after returning from the field. Photographs of 78 birds (we lacked photographs of seven individuals) were taken from several angles using either a Canon DSLR Camera or Apple iPod for



subsequent plumage scoring. Fieldwork was performed with ringing permits obtained from SAFRING, Eswatini's Big Game Parks, Mpumalanga Tourism and Parks Agency, the Cyprus Game and Fauna Service, and with research and collecting permits from the respective authorities (see Acknowledgements).

## ***2.2 Plumage scoring & spectral reflectance***

Methods used to obtain reflectance spectra from forecrown feathers using a spectrophotometer have been described in detail (Nwankwo et al., 2019). In brief, we used a JAZ spectrometer (Ocean Optics) with a fibre-optic reflectance probe (Ocean Optics R-200) and PX xenon light source to obtain two opposite and one perpendicular orientation measurements per set of three to five forecrown feathers from each of 57 individuals for which we collected forecrown feathers. Reflectance spectra were obtained following calibration of the spectrophotometer with a white standard (Ocean Optics WS-1) and dark standard (by covering the fibre-optic connector with its lid). Replicate spectra were averaged in the R package pavo (Maia et al., 2013). Colour variables were estimated using segment classification, following Endler (1990), who divided the spectrum into four equally spaced segments of the tetrachromatic system with ultraviolet, and short-, medium- and long-wavelength sensitive photoreceptors. Although this represents a simplistic approach, segment classification provides results in an intuitive colour space, with angle corresponding to hue and distance from the centre of the colour space to chroma, and these measures (H4 hue and S5 chroma) are provided using `summary.rspec()` in pavo.

Plumage scoring was performed by two project participants who had no experience from the contact zone and hitherto had no involvement in the study (M.M., B.O.O.). They were asked to score forecrown colour of the 78 individuals photographed in the field on an integer scale

from yellow (0) to orange (1) to red (2) from 1,343 photos (mean = 17.2,  $SD = 7.8$  photos per individual). Each individual was photographed several times next to a white standard (Ocean Optics WS-1), or white envelope to aid comparison among photos, except for yellow-fronted tinkerbirds from distantly allopatric populations in Tanzania and individual K69365 from the contact zone. To test whether the same SNPs might otherwise explain other carotenoid-based plumage differences between the species, supercilium colour was also scored from white (0) to cream (1) to yellow (2), and the percentage coverage of yellow over black on the wing bar was also estimated (Figure 1). We then compared scores of the two observers using Spearman rank correlation for each plumage patch; with  $\rho > .85$  for all patches, we averaged the observer's scores for further analysis. For forecrown colour we designated intermediate scores between red and orange as reddish and between orange and yellow as amber. We also compared our qualitative crown scores from photographs with our quantitative values for hue for the 50 individuals for which we had both measurements using Spearman rank correlation to test the reliability of the scoring method, and found they were highly correlated ( $\rho = -.83$ ,  $p = 1.26e^{-13}$ ).

### ***2.3 Raman spectroscopy***

We used Raman spectroscopy to characterize the type of carotenoids present in feathers. We selected forecrown feathers from 11 individuals: two red-fronted and two yellow-fronted from allopatric populations and two of each from sympatric populations, as well as three hybrids. Three Raman spectra with excitation at 785 nm were collected from each feather barb at different positions on the coloured dorsal side of the feather. Raman spectra were obtained using a fibre-optic Raman Probe connected to a 475-mW CW 785-nm Multimode Laser and a FERGIE

1024BRX spectrograph equipped with a 50- $\mu\text{m}$  slit, a 1,200  $\text{mm}^{-1}$  grating (550-nm blaze) and a back-illuminated, deep depletion eXcelon sensor (Teledyne Princeton Instruments). Ten-minute spectra were collected for each position on the feathers without any observed damage.

Cyclohexane was used as a frequency calibration standard. Raman spectra from the same feather sample were averaged together as no distinct difference was observed between the various positions and then smoothed using the Savitzky-Golay filter (Savitzky & Golay, 1964) in matlab R2018a (The MathWorks).

#### ***2.4 DNA extraction and genotyping***

We extracted DNA from blood using a Qiagen QIAmp DNA Blood Mini kit (Qiagen) following the manufacturer's protocols. Extracted DNA was quantified using a NanoDrop (Thermo Scientific 2000c) and a Qubit 2.0 fluorometer with the DNA HS assay kit (Life Technologies). We also checked for DNA quality based on migration on agarose gel, which allowed for the selection of samples with appropriate DNA concentration ( $>20 \text{ ng}/\mu\text{l}$ ) and molecular weight ( $>10,000 \text{ bp}$ ). We sequenced 85 tinkerbird samples using a ddRAD laboratory protocol (Brelsford et al., 2016), which incorporates elements of protocols from previous studies (Parchman et al., 2012; Peterson et al., 2012). Briefly, genomic DNA was digested with restriction enzymes *SbfI* and *MseI* and double-stranded adapters with inline barcodes of 4–8 bp were ligated to the resulting fragments. After magnetic bead purification, the fragments were amplified by PCR in four replicate reactions per individual sample and pooled. We implemented a final purification and size selection of the pooled library using magnetic beads in order to remove primer dimers (and fragments less than 150 bp). Our library was then sequenced on two lanes on the Illumina HiSeq X platform by Novogene Inc., with 150-bp paired-end reads.

## **2.5 Reference genome assembly**

We assembled a low-cost draft genome for *P. p. pusillus*. A single male individual (sample no. AR93139) was selected for assembly, and a short-insert library was prepared by Novogene, Inc., using the NEBNext Ultra II DNA kit (New England Biolabs). The library was sequenced to a depth of approximately 50× on the Illumina HiSeq X platform at Novogene Inc., with 150-bp paired-end reads. Overlapping read pairs were collapsed and adapter and low-quality sequences were removed prior to assembly using pear version 0.9.10 (Zhang et al., 2014) with minimum overlap size 20, minimum read length 30, quality score threshold 20 and maximum proportion of uncalled bases 0.02. We assembled the resulting reads with soapdenovo version 2.04 (Luo et al., 2012) for each odd-numbered value of  $k$  between 41 and 111, with default values for all other parameters. The assembly for  $k = 93$  was chosen on the basis of higher scaffold N50 and assembly length closer to the expected genome size for birds.

We aligned these scaffolds to the zebra finch (*Taeniopygia guttata*) genome using the Nucmer command in mummer 4.0 (Kurtz et al., 2004). Tinkerbird scaffolds aligning to zebra finch chromosomes were ordered and oriented according to these alignments; scaffolds that did not align to the zebra finch genome were ordered by scaffold size..

## **2.6 Single nucleotide polymorphism calling**

Adapter sequences were removed and overlapping paired-end reads merged in pear version 0.9.10 (Zhang et al., 2014) and reads aligned to the *P. p. pusillus* draft genome assembly in bwa mem version 0.7.17 (Li, 2013) using default parameters. Variants were called using bcftools mpileup version 1.8 (Li et al., 2009) with mapping quality  $> 20$  and default values for other parameters. We filtered the resulting variants using vcftools version 0.1.13 (Danecek

et al., 2011), retaining genotypes with depth 4 or greater, and loci with minor allele frequency  $> 0.05$  that were genotyped in at least 80% of individuals.

The SNPs of interest in this study were those most likely to explain differences between red and yellow forecrown colour. samtools has been shown to perform relatively poorly in calling indels (Hwang et al., 2015), so to aid in interpretation of results we also manually inspected genotypes at SNPs most strongly associated with forecrown colour traits as well as at any adjacent indels that may have been incorrectly called using integrative genomics viewer 2.8.9 (Broad Institute, University of California San Diego).

## ***2.7 Genome-wide association analysis***

We tested for an association between each genetic marker and each of the five colour traits (crown hue, chroma and score, and supercilium and wing bar score) using a linear mixed model implemented in gemma 0.94 (Zhou & Stephens, 2012), which uses a relatedness matrix to control for population structure. Because gemma requires loci with no missing data, we imputed missing genotypes using beagle version 5.1 (Browning et al., 2018), based on genotype likelihood scores. Significance was assessed based on a threshold of  $-\log_{10}(\alpha) = 6$ , which results in approximately one expected false positive per trait, taking into account the 104,933 variants tested for each trait. Following Brelsford et al. (2017), we set this significance threshold for consistency across all traits rather than using false discovery rates (FDRs) (Benjamini & Hochberg, 1995), which would result in different significance thresholds per trait. We note that this threshold was approximately in line with the most conservative threshold obtained using FDR, but FDR would also have resulted in significance thresholds as low as  $-\log_{10}(\alpha) = 4$  for certain traits. Scaffolds significantly associated with forecrown colour were then compared with

sequences of candidate genes *CYP2J19* on the zebra finch genome and *BCO2* on the downy woodpecker (*Dryobates pubescens*) genome using BLAST.

## ***2.8 Genetic Sex identification***

We used two complementary methods to sex individuals to investigate relative assortative mating rates of the sexes of each species. One procedure involved the polymerase chain reaction (PCR) using highly conserved primers 2550F and 2718R (Fridolfsson & Ellegren, 1999) to amplify the differently sized introns of Z- and W-linked chromohelicase-DNA binding protein 1 (CHD1) genes. PCR products were separated on a stained 1% or 2% agarose gel run in TAE buffer, revealing one band for male birds and two for females. The other method was a bioinformatics approach where we compared the ratio of average read depth of SNPs from ddRAD sequencing that were aligned with the zebra finch on the Z chromosome with read depths of SNPs on autosomes (see Toews et al., 2018). Because males have two copies and females one copy of the Z chromosome, we would expect a Z:autosome depth ratio of 1 in males and 0.5 in females. Using the two approaches confirmed the accuracy of each method and allowed us to investigate and correct for any possible error if they produced conflicting results.

## ***2.9 Identification of hybrid individuals and direction of backcrossing***

To determine whether individuals with intermediate ancestry were progeny of recent interbreeding or historical events, we used faststructure (Raj et al., 2014) with  $k = 2$  to estimate *pusillus* and *extoni* ancestry (i.e., hybrid index) based on all loci, and separately for loci on scaffolds that aligned to the zebra finch Z chromosome. We estimated interspecific heterozygosity of each individual based on a genome-wide subset of 1,723 SNPs with allele

frequency difference  $> 0.95$  between allopatric *pusillus* and *extoni* populations, and compared this to the hybrid index across the whole genome to identify F<sub>1</sub> hybrids and first-generation backcrosses. Because female birds inherit a single copy of the Z chromosome from their fathers, comparing the Z-chromosome and autosomal hybrid index of hybrids provides information on the direction of backcrossing for early and later-generation backcrosses: a female's Z-chromosome hybrid index should be, on average, equal to her father's Z-chromosome hybrid index, while the same bird's autosomal hybrid index should equal the average of her two parents' hybrid index values. By extension, of the two copies of the Z chromosome in a male, one is entirely descended from his maternal grandfather, while the other reflects a mixture of his two paternal grandparents, in contrast to the autosomes which reflect an average of his four grandparents.

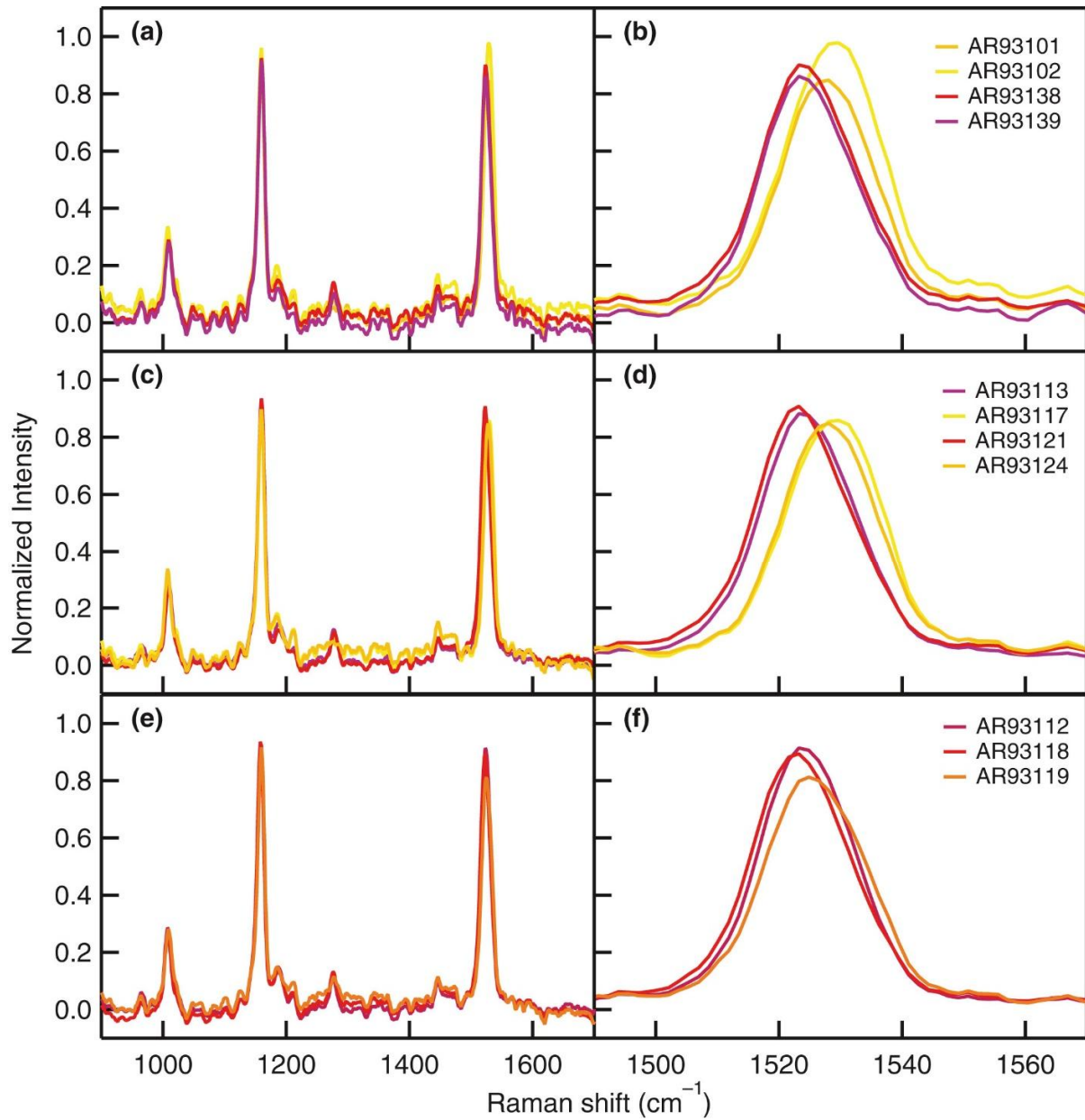
To illustrate the relationship between hybrid index and interspecific heterozygosity, we produced triangle plots, which would reveal F<sub>1</sub> hybrids as individuals with intermediate hybrid index and the highest levels of interspecific heterozygosity ( $>0.7$  based on simulations performed by Toews et al., 2018) at loci diagnostic for each species. F<sub>2</sub> hybrids and backcrosses would be expected to have intermediate levels of interspecific heterozygosity and fall in the middle and sides of the triangle respectively, in accordance with simulations (Toews et al., 2018), with nonadmixed individuals falling in the lower corners of the triangle.

### 3 RESULTS

#### 3.1 Raman spectroscopy

Raman spectra showed three distinct peaks at 1,529–1,523, 1,160 and 1,007–1,009  $\text{cm}^{-1}$ , indicating the presence of carotenoids in forecrown feathers (Figure 2). The spectra of yellow-fronted tinkerbird forecrown feathers showed peaks at 1,527–1,528  $\text{cm}^{-1}$ , associated with C = C stretching of the backbone, 1,160  $\text{cm}^{-1}$  (C–C stretching) and 1,007  $\text{cm}^{-1}$  (in-plane CH rocking, methyl groups attached to the conjugated chain). The spectra for red-fronted tinkerbird forecrown feathers showed a downshift of  $\sim 4 \text{ cm}^{-1}$  in the C=C band to 1,523–1,524  $\text{cm}^{-1}$ , while the other two bands were at 1,160 and 1,009  $\text{cm}^{-1}$  respectively. A further band was observed at 1,278  $\text{cm}^{-1}$  due to a coupled C–H bending mode with C=C stretching along the backbone (Mendes-Pinto et al., 2012). Further differences between yellow and red feathers included a upshift of  $\sim 3 \text{ cm}^{-1}$  in the weaker band at 1,184–1,187  $\text{cm}^{-1}$ , along with a reduction in the intensity of the weak band at 1,211  $\text{cm}^{-1}$ . These are bands associated with C–H bending and C–C stretching (Saito & Tasumi, 1983). The position of the C=C band in particular is very sensitive to the conjugation length in the molecule and follows a dispersion relationship (Veronelli et al., 1995). The presence of carbonyl groups in the  $\beta$ -rings extend the conjugation of the backbone, causing a reduction in the frequency of this band. The Raman spectra of forecrown feathers of hybrid individuals had mixed features: the C=C band appears at 1,523–1,525  $\text{cm}^{-1}$ , which is closer to the band in the red feathers of red-fronted tinkerbird, while the band at 1,185  $\text{cm}^{-1}$  is closer to the band at 1,184  $\text{cm}^{-1}$  observed in yellow feathers of yellow-fronted tinkerbird. Also, a weak band appears at 1,278  $\text{cm}^{-1}$ , as found in the red feathers of red-fronted tinkerbird.





**Figure 2.** Raman spectra of feathers from individuals in (a,b) allopatry: AR93101, AR93102 (yellow-fronted tinkerbirds), AR93138, AR93139 (red-fronted tinkerbirds); (c,d) sympatry: AR93117, AR93124 (yellow-fronted), AR93113, AR93121 (red-fronted); and (e,f) hybrids: AR93112, AR93118, AR93119. Right panels focus on the range encompassing the C=C band shown on the left. Excitation wavelength was 785 nm

### ***3.2 Reference genome assembly***

The assembly for  $k = 93$  resulted in a scaffold N50 of 7.2 kb. The assembled genome spanned 1.16 Gb, and 53% of the assembly was ordered and oriented onto chromosomes on the high-quality zebra finch reference genome (NCBI accession no. SAMN14819987 in BioProject PRJNA630018).

### ***3.3 SNP calling***

We retained 104,933 SNPs at a density of one per 16 kb, with a mean depth of  $19\times$ , and a minor allele frequency  $< 0.05$ , which had been genotyped on at least 80% of the 85 individuals (data accessible from Kirschel, et al., 2020). Of these SNPs, 1,532 were on scaffolds anchored to the Z chromosome, 57,913 were on scaffolds anchored to autosomes and 45,487 were on unplaced scaffolds.

### ***3.4 Genome-wide association analysis***

Admixture mapping revealed a number of genomic regions that were strongly associated with plumage traits that differ between yellow-fronted and red-fronted tinkerbirds (Table 1). After accounting for one expected false positive per trait based on our significance threshold of  $-\log_{10}(\alpha = 6)$ , there were four significant associations of chromosomes with traits. We found that crown colour was significantly associated with two chromosomes. Crown score was significantly associated with SNPs on chromosome 20 (on scaffolds 67410, 67420, 67433 and 67445), and both crown score and crown hue were significantly associated with SNPs on chromosome 8 (Figure 3). Six SNPs on adjacent scaffolds 50344, 50345 and 50346, as well as one on scaffold 50201 on chromosome 8 were significantly associated with crown score, while 14 SNPs on

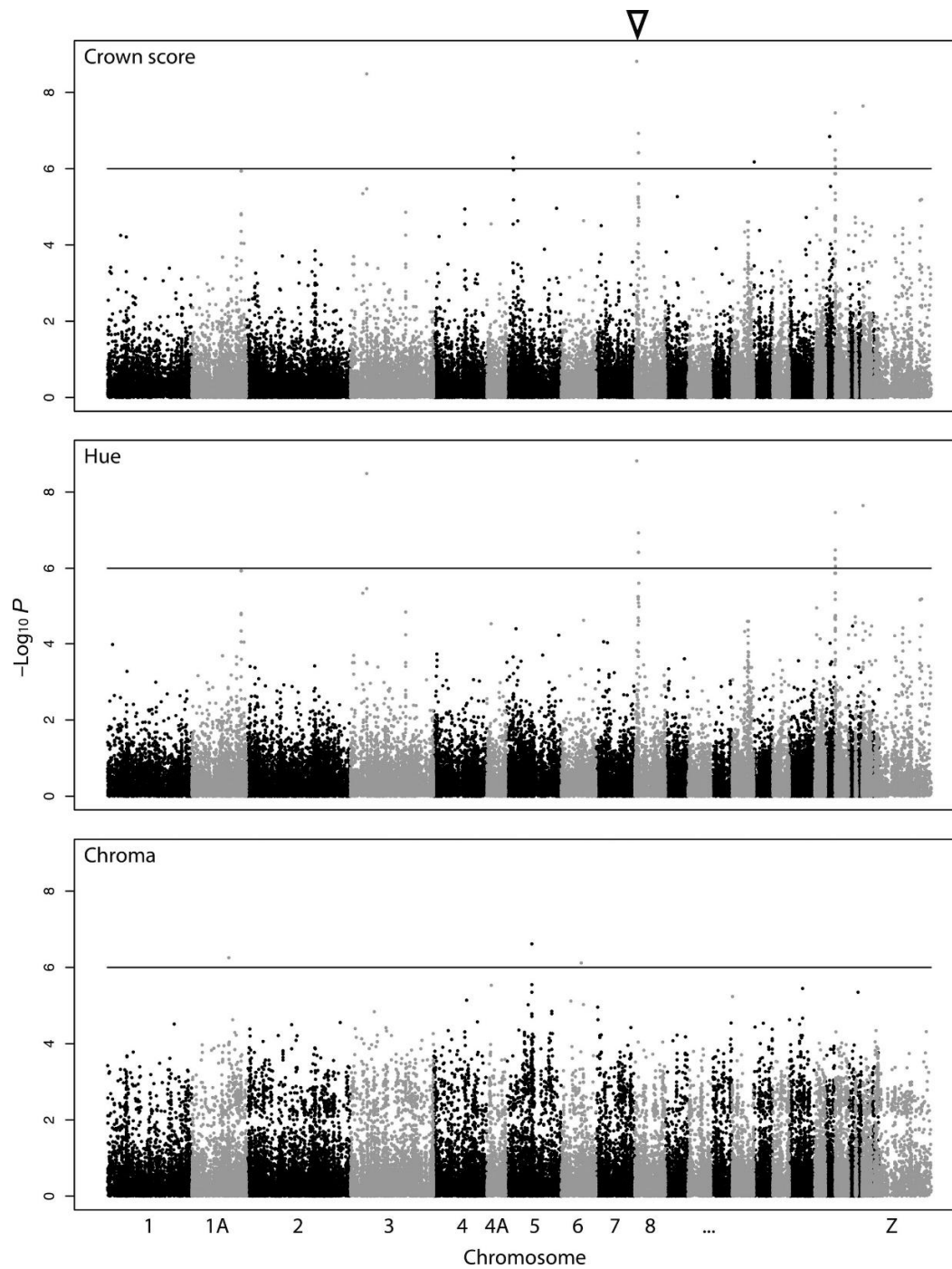
scaffolds 50330, 50337, 50338, 50339 and 50344 on chromosome 8 were significantly associated with crown hue. Indeed, the same SNP on scaffold 50344 on chromosome 8 was significantly associated with both crown hue and crown score (Table S1). The SNP most strongly associated with crown score was on scaffold 50201 on chromosome 8, which aligns to the region 13–21 kb upstream of *CYP2J19A* in zebra finch, and 16–28 kb upstream of cytochrome P450 gene XM\_009910004 in downy woodpecker (manually annotated as *CYP2J19* by Twyman et al., 2018). This scaffold is in fact the one closest located to *CYP2J19A* in zebra finch resulting from our ddRAD sequencing.

**Table 1.** Number of single nucleotide polymorphisms (SNPs) associated with each of eight feather patch traits

Trait	Number of SNPs: $\log_{10}(p) > 6$	Chromosomes with $> 2$ significant SNPs
Crown hue	16	8
Crown chroma	4	None
Crown score	19	8, 20
Wing bar score	1	None
Supercilium score	9	4

Note: Only chromosomes with more than two significant SNPs are shown with associations to each trait because, based on the permutation test, we expect one false positive at  $-\log_{10}(p) > 6$ .

The cluster of SNPs on adjacent scaffolds 50344, 50345 and 50346 on chromosome 8 spans ~150 kb and is located 1.8 Mb from *CYP2J19A* in zebra finch. It overlaps with several other genes in zebra finch: leucine-rich repeat-containing protein 42 (*LRRC42*), intraflagellar transport protein 25 homologue (*HSPB11*), iodothyronine deiodinase 1 (*DIO1*), YIP1 domain family member 1 (*YIPF1*), nucleoporin *NDC1* (*NDC1*), and *GLIS* family zinc finger 1 (*GLIS1*). SNPs associated with crown hue are located 1.4–1.6 Mb from *CYP2J19A* in zebra finch and overlap genes proprotein convertase subtilisin/kexin type 9 (*PCSK9*), Bartter syndrome infantile with sensorineural deafness (*BSND*), Transmembrane protein 61 (*TMEM61*), 24-



**Figure 3.** Manhattan plots for crown score, hue and chroma revealing the region of chromosome 8 significantly associated with red and yellow colour differences (black triangle points to the region). The locus is associated with the *CYP2J19* gene. Black line indicates genome-wide significance at  $-\log_{10}(p) > 6$

dehydrocholesterol reductase (*DHCR24*), proryl tRNA synthetase (*PARS2*), tetratricopeptide repeat domain 4 (*TTC4*), transmembrane protein 205 (*TMEM205*), acyl-coenzyme A thioesterase 11 (*ACOT11*) and single-stranded DNA binding protein 3 (*SSBP3*).

The SNPs on chromosome 20 associated with crown score are located ~1–2 Mb from *ASIP/RALY* on zebra finch, which have been shown to function in plumage coloration (Wang et al., 2019). Those SNPs overlap several genes in zebra finch with no previously known function in pigmentation, specifically PHD finger protein 20 (*PHF20*), chromodomain helicase DNA binding protein 6 (*CHD6*) and homeobox protein *TGIF2*, but also retinoblastoma-like protein 1 (*RBL1*), which has recently been shown to affect black skin pigmentation in mice (Naert et al., 2020). There were no chromosomes with more than two significant SNPs associated with crown chroma or wing bar percentage of yellow over black, but we did find a significant association with regions of the genome and supercilium score, associated with chromosome 4 (Table 1, Table S1) with SNPs overlapping genes *C4H20orf194* and potassium voltage-gated channel interacting protein 4 (*KCNIP4*).

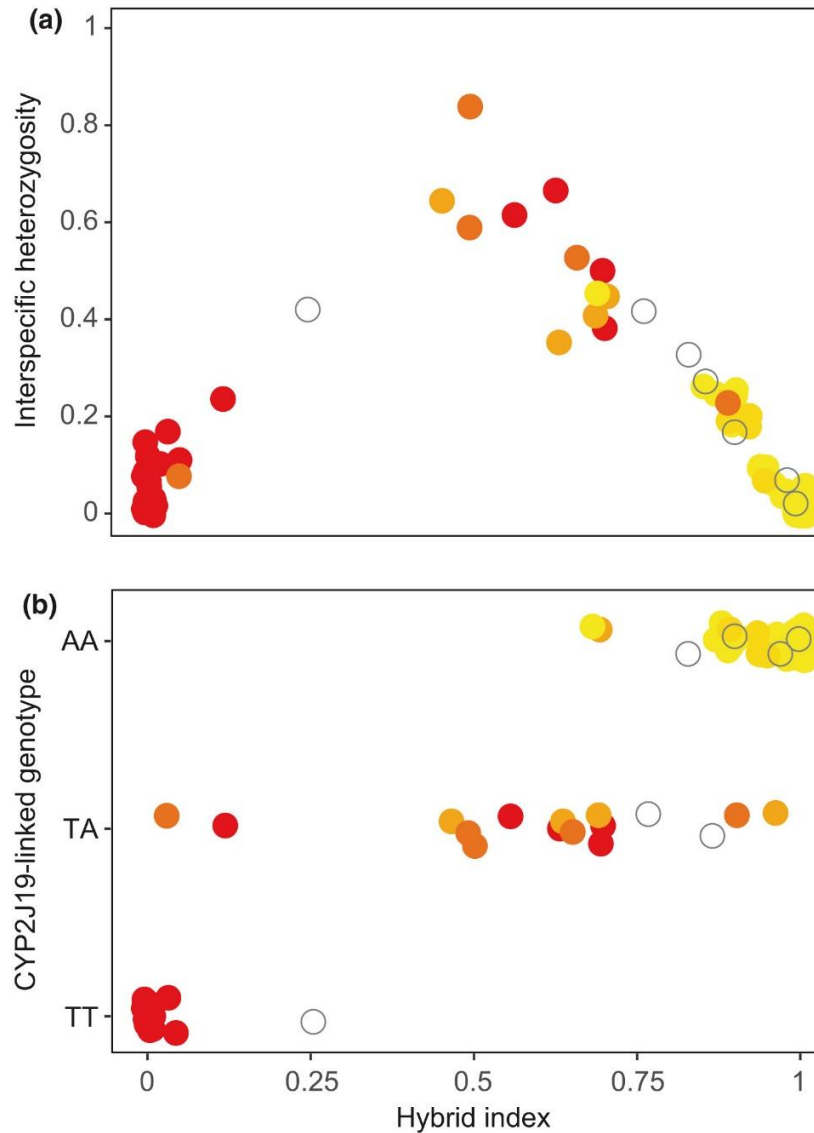
### ***3.5 Sex determination***

Using PCR and bioinformatics approaches, we identified 48 males and 37 females across the contact zone. The bioinformatics approach involved comparing the mean depth on 1,533 SNPs on the Z chromosome with 103,401 other SNPs for each individual. We expected comparatively higher Z chromosome to autosome depth ratios for males compared to females, and we indeed found a clear separation. Male Z:autosome ratios ranged from 0.83 to 1.19, while female ratios ranged from 0.43 to 0.67 (see Supporting Information). The results of the bioinformatics method

corresponded 100% with the PCR and gel electrophoresis method of Fridolfsson and Ellegren (1999).










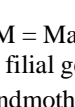
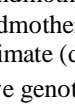
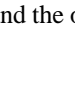
### 3.6 Identification of hybrid individuals and direction of backcrossing

Out of 49 individuals sampled in the contact zone, 14 were admixed at the level between first-generation backcrosses (with a hybrid index between ~0.2 and 0.8, Figure 4a). Among the 14 admixed individuals we identified one F<sub>1</sub> hybrid (AR93112) with interspecific heterozygosity > 0.7 (Toews et al., 2018), while the remaining hybrids probably had more complex ancestry (Table 2). Backcrossing thus appeared asymmetric: autosomes of admixed individuals had, on average, a higher percentage of *extoni* compared to *pusillus* genotype than the Z chromosome based on their respective hybrid index (Table 2). This suggests that hybrids result from females that have a higher proportion of *extoni* ancestry mating with males with a relatively higher proportion of *pusillus* ancestry than the other way around, as found in nine of 14 individuals (compared to three with the reverse pattern and two with equal ancestry). For instance, female AR93167 had autosomal and Z hybrid indexes of 0.559 and 0.000 respectively, with an *extoni* mitochondrial haplotype (Table 2). With over 50% *extoni* autosomal hybrid index (and *extoni* mtDNA haplotype), her mother was probably a “pure” *extoni* and her father mostly *pusillus* (Table 2).



**Figure 4.** Forecrown colour score, represented by dot colour (scale: red-reddish-orange-amber-yellow) in relation to hybrid index on a scale from 0 (*Pogoniulus p. pusillus* genotype) to 1 (*P. c. extoni* genotype), and (a) interspecific heterozygosity, and (b) genotype of a single nucleotide polymorphism (SNP) linked to *CYP2J19* on scaffold 50201 on chromosome 8. Grey circles represent individuals which were not photographed, but for which crown feathers were analysed using reflectance spectrophotometry. While nonhybrids homozygous for their respective allele are characterized by species-specific forecrown colour, individuals heterozygous at the *CYP2J19*-linked SNP have orange to red forecrowns, even in *extoni* genotypes with little admixture evident. Backcrosses are mostly into *extoni*

**Table 2:** Admixed individuals, their autosomal hybrid index, Z-chromosome hybrid index, interspecific heterozygosity, mtDNA haplotype, sex, and their putative parents, with putative grandparents implied from order given when two genotypes shown (mother then father), except where shown. Banner shows photos of forecrown for each individual except AR93119.

individual	inter-				sex <sup>†</sup>	putative mother <sup>‡</sup>	putative father
	hybrid index autosomes	hybrid index Z chromos.	specific hetero-zygosity	mtDNA haplotype			
AR93112		0.498	0.495	0.84	<i>extoni</i>	M	<i>extoni</i> / <i>pusillus</i>
AR93115		0.681	1.000	0.41	<i>pusillus</i>	F	F1 x <i>pusillus</i> BC <sup>§</sup> / <i>extoni</i>
AR93118		0.493	0.210	0.60	<i>extoni</i>	M	<i>extoni</i> x <i>pusillus</i> / <i>extoni</i> x <i>pusillus</i> <sup>¶</sup>
AR93122		0.689	0.097	0.46	<i>extoni</i>	F	<i>extoni</i> / F1 x <i>pusillus</i> BC
AR93153		0.696	0.878	0.37	<i>extoni</i>	F	F2 / <i>extoni</i> x <i>extoni</i> BC <sup>¶</sup>
AR93157		0.632	0.417	0.36	<i>extoni</i>	M	<i>extoni</i> BC x F1 / F1 x <i>extoni</i> BC
AR93159		0.629	0.490	0.66	<i>extoni</i>	M	<i>extoni</i> BC / <i>extoni</i> x <i>pusillus</i> <sup>¶</sup>
AR93167		0.559	0.000	0.61	<i>extoni</i>	F	<i>extoni</i> / <i>pusillus</i> BC x <i>pusillus</i>
AR93168		0.695	0.284	0.51	<i>extoni</i>	F	<i>extoni</i> / <i>pusillus</i> BC x F1
AR93170		0.695	0.645	0.46	<i>extoni</i>	M	<i>extoni</i> / <i>pusillus</i> BC x F1
AR93172		0.647	0.260	0.53	<i>extoni</i>	F	<i>extoni</i> / <i>pusillus</i> BC
K69365		0.459	0.000	0.65	<i>extoni</i>	F	<i>extoni</i> x <i>extoni</i> BC / <i>pusillus</i>
AR93119		0.249	0.250	0.41	<i>extoni</i>	M	F2 / <i>pusillus</i>

<sup>†</sup>F = Female, M = Male.

<sup>‡</sup>F1 is the first filial generation offspring hybrid, F2 second filial generation offspring hybrid, BC = backcross.

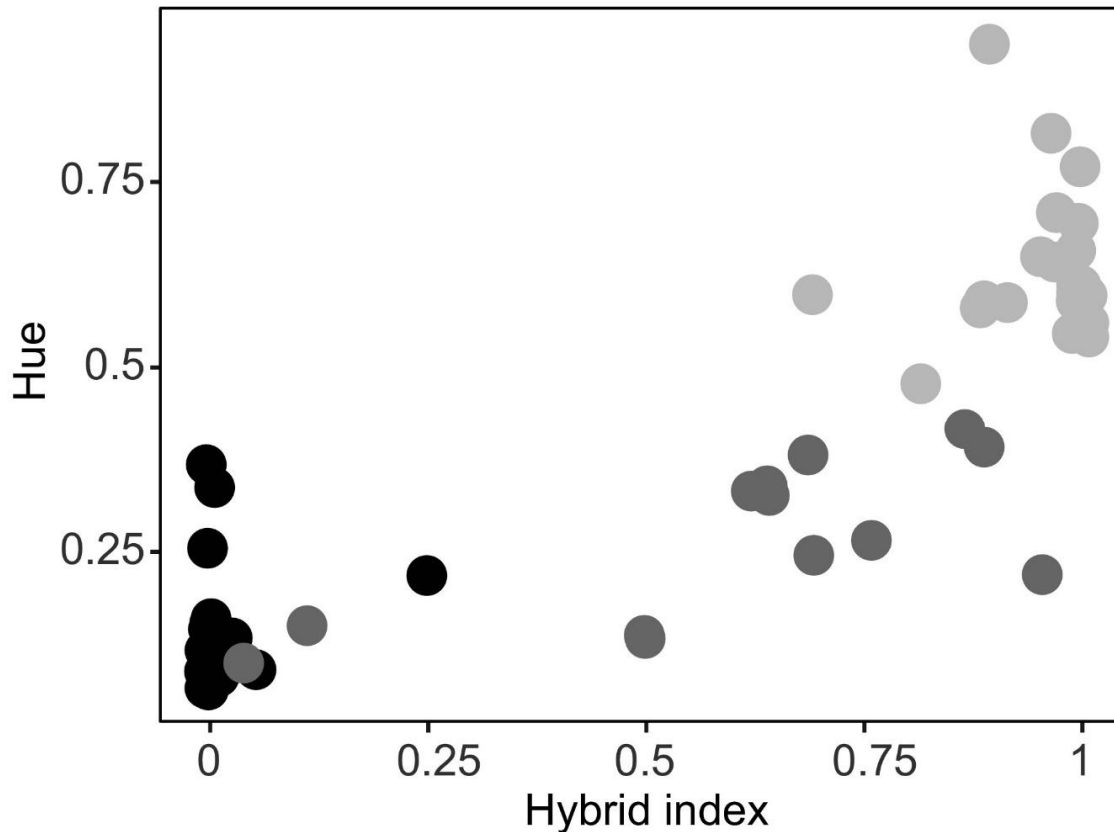
<sup>§</sup>Maternal grandmother could have been an F1 with maternal grandfather a *pusillus* backcross or vice versa, but the maternal grandmother's mother will have carried a *pusillus* haplotype either way. Putative parents and grandparents are all approximate (do not account for recombination), but consistent with the hybrid index values.

<sup>¶</sup>The respective genotypes of the paternal grandfather and grandmother cannot be determined, only that one was likely *extoni* and the other *pusillus* (or an F1 for AR93153).



### ***3.7 Forecrown plumage and CYP2J19***

Closer inspection of the SNP most closely associated with forecrown colour score at position 7463 on scaffold 50201 on chromosome 8 revealed some incorrect calls, which once corrected revealed an even closer association with forecrown colour. All individuals homozygous for the *pusillus* allele at this locus were scored with red forecrowns, while heterozygotes were scored red, reddish or orange, regardless of their hybrid index (Figure 4b). Forecrown score of homozygotes with the *extoni* allele ranged from yellow and amber for nonadmixed individuals to orange for a hybrid (AR93170, but which is heterozygous at several other significant SNPs on chromosome 8 that we examined; see Supporting Information). After correcting variant calls, we could also see a very clear relationship between the genotype at the *CYP2J19* locus and crown hue. All heterozygotes at the locus had redder hues than homozygotes at the locus with comparative hybrid index (Figure 5).



**Figure 5.** Forecrown hue in relation to hybrid index. Dot shade represents the genotype at the variant on scaffold 50201 linked to *CYP2J19*, with the (T/T) homozygote in black, (A/A) in light grey and the heterozygote in dark grey. Individuals homozygous for the red allele or heterozygous at the locus have nonoverlapping hue with individuals homozygous for the yellow allele. Strikingly, all individuals heterozygous at the locus have redder hue (with hue < 0.5) than all individuals homozygous for the yellow allele (with hue > 0.5) at equivalent hybrid indexes

#### 4 DISCUSSION

We found that *CYP2J19* on chromosome 8 was within one of two regions associated with crown colour across a natural hybrid zone in tinkerbirds. Indeed, it was the only region of the genome that was significantly associated with both hue, determined from spectral reflectance, and forecrown plumage colour score. All *extoni* individuals homozygous for the yellow-fronted

*CYP2J19*-linked SNP exhibited a yellow forecrown and all individuals homozygous for the red-fronted allele had red forecrowns, regardless of their ancestry. All heterozygotes at the *CYP2J19*-linked locus had either red, reddish or orange crowns. *CYP2J19* is a cytochrome P450 enzyme, which has been implicated as encoding the ketolase that mediates red coloration in birds (Lopes et al., 2016; Mundy et al., 2016). Ketolases convert dietary yellow carotenoids into red ketocarotenoids in birds with red feathers (Norden & Price, 2018; Toews et al., 2017).

Peak shifts in our Raman spectra of red and yellow tinkerbird feathers, especially the downshift of the strong C=C stretching band and the presence of the band at  $1,278\text{ cm}^{-1}$  in red feathers is consistent with findings in previous Raman studies (Thomas, et al., 2014; Veronelli et al., 1995). They suggest the conversion of a yellow dietary carotenoid such as lutein to ketocarotenoid  $\alpha$ -doradexanthin, both of which have been associated with yellow and red feather colour in Piciformes (Stradi et al., 1998; Thomas, et al., 2014). Indeed, comparison of our Raman spectra with those of related toucans, where  $\alpha$ -doradexanthin was the primary pigment identified in red feathers (Thomas & James, 2016), reveals remarkable concordance. Spectral peaks corresponded both in the frequencies of the C=C and C–C bands ( $1,523$  and  $1,160\text{ cm}^{-1}$  respectively) as well as in lower intensity bands in the  $1,100$ – $1,400\text{ cm}^{-1}$  fingerprint region associated with the C–C stretching and C–H bending coupled vibrations (see LaFountain et al., 2015). Our results are thus consistent with  $\alpha$ -doradexanthin as the primary ketocarotenoid detected in red tinkerbird feathers as opposed to those with increased effective conjugation lengths, such as canthaxanthin, for example in *Apaloderma narina* with peaks for C–C and C=C bands at  $1,155$  and  $1,510\text{ cm}^{-1}$  respectively (Thomas & James, 2016), and astaxanthin (Veronelli et al., 1995).

The metabolic pathway for  $\alpha$ -doradoxanthin involves C(4) oxygenation of lutein (LaFountain et al., 2015), suggesting lutein is the dietary carotenoid present in yellow forecrown feathers of tinkerbirds. The closest relative of tinkerbirds with yellow feathers analysed with Raman spectroscopy, the distantly related *Colaptes auratus* (Thomas & James, 2016), does not perfectly correspond with what we find in tinkerbirds (C=C band peak at  $1,524\text{ cm}^{-1}$ , compared with  $1,527\text{--}1,528\text{ cm}^{-1}$  for yellow forecrown in tinkerbirds). However, *C. auratus* has a high proportion of the carotenoids  $\beta$ -carotene and zeaxanthin present in its feathers (Hudon et al., 2015), represented by increased effective conjugation lengths, in addition to lutein (Thomas, et al., 2014). The differences are probably because *C. auratus* feeds primarily on ants, which contain mostly  $\beta$ -carotene and only traces of lutein (Hudon et al., 2015). Tinkerbirds, by contrast, are primarily frugivores (Hockey et al., 2005), and lutein occurs in high concentrations in fruit (Sommerburg et al., 1998).

The Raman spectra of feathers from hybrid individuals show intermediate features to those of yellow and red feathers, which suggests the presence of a mixture of the two pigments, potentially explaining the presence of orange and reddish crowns in hybrids. Heterozygotes at *CYP2J19* might deposit both dietary carotenoids and ketocarotenoids in their feathers, but further work using high performance liquid chromatography (HPLC) would be required to test this. *CYP2J19* has also been associated with red retinal oil droplets influencing colour vision in birds (Mundy et al., 2016), proposed to be its ancestral function, with its role in red coloration having evolved in some but not other species (Twyman, et al., 2018). It has also been shown to function in red integumental coloration in turtles (Twyman et al., 2016).

Both quantitative (hue) and qualitative (crown score) metrics recovered the same major-effect locus. This might not be surprising if they are both measures of the same trait, but each

method has its own inherent biases. Scoring from photographs is subjective and affected by each observer's perspective of the effects of ambient light. While highly correlated, there was variation in their respective scores. Likewise, reflectance spectrometry is susceptible to variation in feather and probe placement, although we did attempt to control for this with measurements in three orientations. Despite these potential biases in qualitative and quantitative metrics, and that just 50 of 85 samples were used in both analyses, the same major-effect locus was recovered. Furthermore, we showed that admixture mapping is feasible using RADseq with a sample size ~50, as was shown for forecrown hue, but only for major-effect loci. This was possible in spite of no prior genomic resources available for *Pogoniulus* tinkerbirds or from any closely related genera.

*CYP2J19* is not the only gene shown to function in red coloration in birds, however, with recent work finding that a mutation in *BCO2* functions in red bare part coloration (Gazda, et al., 2020). *BCO2* is on chromosome 24, and a single SNP on scaffold 70216 on chromosome 24 was significantly associated with crown score here, but with just one SNP associated, the chromosome did not pass our significance threshold. Furthermore, the SNP aligned to the interval from 5.8 to 6.0 Mb on zebra finch chromosome 24, while *BCO2* spans from 1.53 to 1.54 Mb, suggesting that the SNP associated with forecrown colour might not be linked to *BCO2*, notwithstanding the possibility that a higher marker density might reveal a closer association. The *CYP2J19*-linked SNP was not the only region associated with red forecrown colour in tinkerbirds, with chromosome 20 associated with crown score. Those SNPs were also 1–2 Mb away from the *ASIP-RALY* block known to play a role in pigmentation (Nadeau et al., 2008), but were in a region of chromosome 20 associated with supraloral and post-ocular plumage coloration in yellow-rumped warbler *Setophaga coronata* (Brelsford et al., 2017). Most

other genes that significant SNPs overlapped with have no previously known function in pigmentation, except for *RBL1*, shown to affect skin pigmentation in mice (Naert et al., 2020).

We found that forecrown colour could be intermediate between red and yellow, with some heterozygotes at the *CYP2J19* locus displaying orange forecrowns. While genotyping variants not completely linked to the causal locus might explain some of the variation found, the association of heterozygotes at the linked locus with intermediate crown colour might suggest possible additive effects of the gene rather than dominance of one allele over the other, and/or interactions with genes at other regions we found associated with forecrown colour. Previous work on carotenoid content in red and yellow feathers of the Piciform *Colaptes cafer* and *C. auratus* across a hybrid zone using HPLC found that intermediate colours in hybrids represented incomplete oxygenation between dietary carotenoids and ketocarotenoids (Hudon et al., 2015), and a recent study suggests colour differences are associated with *CYP2J19* across that hybrid zone (Aguillon et al., 2020).

We found no significant association with crown chroma. Unlike in hue, the two species were shown to overlap in chroma between sympatric forms by Nwankwo et al. (2019). However, we did find SNPs significantly associated with supercilium colour, but not the extent of yellow on the wing bar. The SNPs associated with supercilium colour were on a different chromosome to those associated with forecrown colour, indicating that a different pathway is involved in mediating carotenoid-based coloration in those traits. This is not unexpected. The supercilium varies between white and shades of yellow, while *CYP2J19* has been shown to function in red feather colour determination (Lopes et al., 2016; Mundy et al., 2016). Wing bar colour, by contrast, has been known to be reddish in *pusillus* (A. Kirschel unpubl. data) and future work will hopefully elucidate the pathway that explains such reddish colour in the wing. We

acknowledge that limitations of marker density with our ddRADseq approach might mean we have missed associations with some traits.

In another pair of sister taxa of *Pogoniulus* tinkerbird, yellow-rumped (*P. bilineatus*) and yellow-throated tinkerbird (*P. subsulphureus*), which meet in the forests of west and central Africa, reproductive isolation is maintained through character differences, such as in song and throat colour, which have diverged in sympatry (Kirschel et al., 2009, 2020). By contrast, yellow-fronted and red-fronted tinkerbird hybridize extensively, and hybridization is asymmetric (Nwankwo et al., 2019). Based on the high proportion of individuals with *extoni* (i.e., yellow-fronted) genotypes but red forecrowns in the contact zone (Nwankwo et al., 2019), even when female *pusillus* mate with males with a high proportion of *extoni* ancestry, those males may still sport reddish forecrowns. Asymmetry between mitochondrial haplotype and genotype at *CYP2J19* could result from a genetic incompatibility in the reverse cross (i.e., *pusillus* haplotype females interbreeding with yellow-fronted males). Such mitonuclear incompatibilities could affect carotenoid oxidation and feather pigmentation, with coloration thus signalling the quality of cellular function (Hill et al., 2019). Yet, such crosses do occur—two individuals in our sample with *pusillus* haplotype had *extoni* fathers (AR93115 and AR93163); both individuals are females, the heterogametic sex, and thus theoretically more likely to suffer from inviability and infertility (Haldane, 1922). While asymmetry may still result from lower intrinsic or extrinsic fitness in the *pusillus* female  $\times$  *extoni* male cross, we instead suggest the asymmetry is a consequence of female preference for males with red forecrowns in *pusillus* and potentially in *extoni* females (cf. Baldassarre et al., 2014). The *pusillus* mitochondrial haplotype is less than one third as common as *extoni* in the contact zone (14/49 individuals, see Nwankwo et al. (2019), supporting information). Yet female *pusillus* appear to put the extra effort into

finding *pusillus* haplotype males, outnumbered by their *extoni* haplotype counterparts. By contrast, female *extoni* appear to breed with males of either genotype at rates equivalent to their frequency in the population. Mate choice experiments would be needed to test whether female *extoni* would choose male *pusillus* (or otherwise male *extoni* with introgressed red forecrowns) over yellow-fronted male *extoni*, when given a choice. However, it does appear to be the failure of female *extoni* to mate assortatively with males of their own species and phenotype that probably drives introgressive hybridization between these species. Premating isolation between the two species remains weak in spite of 4 million years of divergence (Nwankwo et al., 2019).

Red feathers result from the conversion of dietary carotenoids to red ketocarotenoids and such converted carotenoids have been shown to be an honest indicator of fitness that could function in mate choice (Weaver et al., 2018). Here, female *pusillus* might only mate with males with red forecrowns because they consider males with yellower hues to be of lower quality. Greater extents of difference in plumage between related species have been proposed to play a role in pre-mating isolation (Scordato et al., 2017). Here, however, yellow-fronted females instigate asymmetric introgression by not mating assortatively with yellow-fronted males. Red forecrowns are probably a derived trait according to the mtDNA phylogeny (Nwankwo et al., 2019), and if there was a sensory bias for red plumage coloration the two species would surely collapse into one if there is no loss of fitness in hybrids. With heterozygotes at the *CYP2J19* locus displaying more reddish forecrowns, we would also expect red plumage to rapidly introgress across the population. However, we should also bear in mind other factors that could affect the introgression rate and location of the hybrid zone, including dispersal distance, habitat barriers and historical vicariance. Further work is needed to determine the extent to which



species boundaries are maintained and the rate of introgression of red plumage across the contact zone.

## **5 CONCLUSION**

We performed a GWAS to investigate which genes may underlie differences between red and yellow feathers in tinkerbirds. We found an association with *CYP2J19* on chromosome 8. To our knowledge, this is the first time such an association has been found with feather colour across a natural avian hybrid zone, and indeed the first time *CYP2J19* has been associated with red feather colour in a nonpasserine bird. Asymmetric hybridization suggests a preference for red plumage in females that share the red trait, consistent with converted carotenoids reflecting male fitness.

## **ACKNOWLEDGEMENTS**

We thank Louis Hadjioannou, Kim Mortega, Mnqobi Mamba, Maneno Mbilinyi and Phumlile Simelane for assistance in the field, Alan Howland, Colleen Downs, David Eilers-Smith, Matt and Stephanie McGinn, John and Retha Harding, and Neil Baker and the late Liz Baker for assistance with logistics, and Andrea Fulgione and three anonymous reviewers for helpful comments on the manuscript. We thank The Kingdom of Eswatini's Big Game Parks, Ezemvelo KZN Wildlife, Tanzania Wildlife Research Institute (TAWIRI), Tanzania Commission for Science and Technology (COSTECH), Tanzania National Parks (TANAPA), and Mpumalanga Tourism and Parks Agency for research permits. Funding was provided by FP7 Marie Curie Reintegration Grant No. 268316 and a University of Cyprus Research Grant (A.N.G.K.), an AG

Leventis Foundation grant (M.M.) and by the AP Leventis Ornithological Research Institute, Jos, Nigeria (E.C.N. and B.O.O.).

## **DATA ACCESSIBILITY**

The *Pogoniulus pusillus* genome assembly has been deposited at NCBI SRA in BioProject PRJNA630018, with DDRAD sequencing reads under BioProject PRJNA666541. The master VCF file and gemma and R Code have been deposited in the Dryad Digital Repository (<https://doi-org.uplib.idm.oclc.org/10.5061/dryad.jm63xsj87>).

## **AUTHOR CONTRIBUTIONS**

A.N.G.K. conceived the study and designed it with A.M., S.C.H. and A.B.; A.N.G.K. and E.C.N. performed fieldwork with help from A.M.; E.C.N., D.P., M.M. and B.O.O. performed molecular labwork; E.C.N. performed spectrophotometry; M.M. and B.O.O. scored plumage traits; S.M.L. performed Raman spectroscopy under supervision from S.C.H.; A.B. assembled the reference genome and performed bioinformatics with B.O.O., S.M.L. and A.N.G.K.; A.B., E.C.N., S.M.L., S.C.H. and A.N.G.K. analysed data; and A.N.G.K. wrote the manuscript with contributions from all authors.

## **REFERENCES**

- Aguillon, S. M., Walsh, J., & Lovette, I. J. (2020). Extensive hybridization reveals multiple coloration genes underlying a complex plumage phenotype. *bioRxiv*, preprint. <https://doi.org/10.1101/2020.07.10.197715>
- Andersson, S., Prager, M., & Johansson, E. I. A. (2007). Carotenoid content and reflectance of yellow and red nuptial plumages in widowbirds (*Euplectes* spp.). *Functional Ecology*, 21(2), 272– 281. <https://doi.org/10.1111/j.1365-2435.2007.01233.x>

- Baldassarre, D. T., White, T. A., Karubian, J., & Webster, M. S. (2014). Genomic and morphological analysis of a semipermeable avian hybrid zone suggests asymmetrical introgression of a sexual signal. *Evolution*, 68(9), 2644– 2657. <https://doi.org/10.1111/evo.12457>
- Benjamini, Y., & Hochberg, Y. (1995). Controlling the false discovery rate—A practical and powerful approach to multiple testing. *Journal of the Royal Statistical Society Series B-Statistical Methodology*, 57(1), 289– 300. <https://doi.org/10.1111/j.2517-6161.1995.tb02031.x>
- Billerman, S. M., Cicero, C., Bowie, R. C. K., & Carling, M. D. (2019). Phenotypic and genetic introgression across a moving woodpecker hybrid zone. *Molecular Ecology*, 28(7), 1692– 1708. <https://doi.org/10.1111/mec.15043>
- Birkhead, T. (2008). *The wisdom of birds: An illustrated history of ornithology*. London, UK: Bloomsbury.
- Brelsford, A., Dufresnes, C., & Perrin, N. (2016). High-density sex-specific linkage maps of a European tree frog (*Hyla arborea*) identify the sex chromosome without information on offspring sex. *Heredity*, 116(2), 177– 181. <https://doi.org/10.1038/hdy.2015.83>
- Brelsford, A., Toews, D. P. L., & Irwin, D. E. (2017). Admixture mapping in a hybrid zone reveals loci associated with avian feather coloration. *Proceedings of the Royal Society B-Biological Sciences*, 284(1866), 20171106. <https://doi.org/10.1098/rspb.2017.1106>
- Browning, B. L., Zhou, Y., & Browning, S. R. (2018). A one-penny imputed genome from next-generation reference panels. *The American Journal of Human Genetics*, 103(3), 338– 348. <https://doi.org/10.1016/j.ajhg.2018.07.015>
- Brush, A. H. (1970). Pigments in hybrid, variant and melanic tanagers (birds). *Comparative Biochemistry and Physiology*, 36(4), 785– 793. [https://doi.org/10.1016/0010-406x\(70\)90533-5](https://doi.org/10.1016/0010-406x(70)90533-5)
- Campagna, L., Repenning, M., Silveira, L. F., Fontana, C. S., Tubaro, P. L., & Lovette, I. J. (2017). Repeated divergent selection on pigmentation genes in a rapid finch radiation. *Science Advances*, 3(5), E1602404. <https://doi.org/10.1126/sciadv.1602404>
- Danecek, P., Auton, A., Abecasis, G., Albers, C. A., Banks, E., DePristo, M. A., Handsaker, R. E., Lunter, G., Marth, G. T., Sherry, S. T., McVean, G., & Durbin, R. (2011). The variant call format and VCFtools. *Bioinformatics*, 27(15), 2156– 2158. <https://doi.org/10.1093/bioinformatics/btr330>
- del Hoyo, J., Elliott, A. J. S., Christie, D. A., & Kirwan, G. (2020). *Handbook of the birds of the world alive*. Barcelona, Spain: Lynx Edicions.
- Delmore, K. E., Toews, D. P. L., Germain, R. R., Owens, G. L., & Irwin, D. E. (2016). The genetics of seasonal migration and plumage color. *Current Biology*, 26(16), 2167– 2173. <https://doi.org/10.1016/j.cub.2016.06.015>

- Dowsett-Lemaire, F. (1988). Fruit choice and seed dissemination by birds and mammals in the evergreen forests of upland Malawi. *Revue D'écologie*, 43, 251– 285.
- Endler, J. A. (1990). On the measurement and classification of colour in studies of animal colour patterns. *Biological Journal of the Linnean Society*, 41(4), 315– 352.  
<https://doi.org/10.1111/j.1095-8312.1990.tb00839.x>
- Fridolfsson, A. K., & Ellegren, H. (1999). A simple and universal method for molecular sexing of non-ratite birds. *Journal of Avian Biology*, 30(1), 116– 121. <https://doi.org/10.2307/3677252>
- Gazda, M. A., Araújo, P. M., Lopes, R. J., Toomey, M. B., Andrade, P., Afonso, S., Marques, C., Nunes, L., Pereira, P., Trigo, S., Hill, G. E., Corbo, J. C., & Carneiro, M. (2020). A genetic mechanism for sexual dichromatism in birds. *Science*, 368(6496), 1270– 1274.  
<https://doi.org/10.1126/science.aba0803>
- Gazda, M. A., Toomey, M. B., Araújo, P. M., Lopes, R. J., Afonso, S., Myers, C. A., Serres, K., Kiser, P. D., Hill, G. E., Corbo, J. C., & Carneiro, M. (2020). Genetic basis of De Novo appearance of carotenoid ornamentation in bare parts of canaries. *Molecular Biology and Evolution*, 37(5), 1317– 1328. <https://doi.org/10.1093/molbev/msaa006>
- Godschalk, S. K. B. (1985). Feeding-behavior of avian dispersers of mistletoe fruit in the loskopdam-nature-reserve, South-Africa. *South African Journal of Zoology*, 20(3), 136– 146.
- Haas, F., Pointer, M. A., Saino, N., Brodin, A., Mundy, N. I., & Hansson, B. (2009). An analysis of population genetic differentiation and genotype-phenotype association across the hybrid zone of carrion and hooded crows using microsatellites and MC1R. *Molecular Ecology*, 18(2), 294– 305. <https://doi.org/10.1111/j.1365-294X.2008.04017.x>
- Haldane, J. B. S. (1922). Sex ratio and unisexual sterility in hybrid animals. *Journal of Genetics*, 7, 101– 109. <https://doi.org/10.1007/BF02983075>
- Harrison, R. G., & Larson, E. L. (2016). Heterogeneous genome divergence, differential introgression, and the origin and structure of hybrid zones. *Molecular Ecology*, 25(11), 2454– 2466. <https://doi.org/10.1111/mec.13582>
- Hill, G. E., Hood, W. R., Ge, Z., Grinter, R., Greening, C., Johnson, J. D., Park, N. R., Taylor, H. A., Andreasen, V. A., Powers, M. J., Justyn, N. M., Parry, H. A., Kavazis, A. N., & Zhang, Y. (2019). Plumage redness signals mitochondrial function in the house finch. *Proceedings of the Royal Society B: Biological Sciences*, 286(1911), 20191354.  
<https://doi.org/10.1098/rspb.2019.1354>
- Hill, G. E., & McGraw, K. J. (2004). Correlated changes in male plumage coloration and female mate choice in cardueline finches. *Animal Behaviour*, 67(1), 27– 35.  
<https://doi.org/10.1016/j.anbehav.2003.02.002>

Hockey, P. A. R., Dean, W. R. J., & Ryan, P. (2005). Roberts birds of Southern Africa ( 7th ed.). Cape Town, South Africa: Trustees of the John Voelcker Bird Book Fund.

Hoekstra, H. E. (2006). Genetics, development and evolution of adaptive pigmentation in vertebrates. *Heredity*, 97(3), 222– 234. <https://doi.org/10.1038/sj.hdy.6800861>

Hooper, D. M., Griffith, S. C., & Price, T. D. (2019). Sex chromosome inversions enforce reproductive isolation across an avian hybrid zone. *Molecular Ecology*, 28(6), 1246– 1262. <https://doi.org/10.1111/mec.14874>

Hudon, J., Wiebe, K. L., Pini, E., & Stradi, R. (2015). Plumage pigment differences underlying the yellow-red differentiation in the Northern Flicker (*Colaptes auratus*). *Comparative Biochemistry and Physiology Part B: Biochemistry and Molecular Biology*, 183, 1– 10. <https://doi.org/10.1016/j.cbpb.2014.12.006>

Hwang, S., Kim, E., Lee, I., & Marcotte, E. M. (2015). Systematic comparison of variant calling pipelines using gold standard personal exome variants. *Scientific Reports*, 5(1), 17875. <https://doi.org/10.1038/srep17875>

Kearns, A. M., Restani, M., Szabo, I., Schröder-Nielsen, A., Kim, J. A., Richardson, H. M., Marzluff, J. M., Fleischer, R. C., Johnsen, A., & Omland, K. E. (2018). Genomic evidence of speciation reversal in ravens. *Nature Communications*, 9(1), 906. <https://doi.org/10.1038/s41467-018-03294-w>

Kim, K.-W., Jackson, B. C., Zhang, H., Toews, D. P. L., Taylor, S. A., Greig, E. I., Lovette, I. J., Liu, M. M., Davison, A., Griffith, S. C., Zeng, K., & Burke, T. (2019). Genetics and evidence for balancing selection of a sex-linked colour polymorphism in a songbird. *Nature Communications*, 10(1), 1852. <https://doi.org/10.1038/s41467-019-09806-6>

Kirschel, A. N. G., Blumstein, D. T., & Smith, T. B. (2009). Character displacement of song and morphology in African tinkerbirds. *Proceedings of the National Academy of Sciences of the United States of America*, 106(20), 8256– 8261. <https://doi.org/10.1073/pnas.0810124106>

Kirschel, A. N. G., Nwankwo, E. C., & Gonzalez, J. C. T. (2018). Investigation of the status of the enigmatic White-chested Tinkerbird *Pogoniulus makawai* using molecular analysis of the type specimen. *Ibis*, 160(3), 673– 680. <https://doi.org/10.1111/ibi.12597>

Kirschel, A. N. G., Nwankwo, E. C., Pierce, D., Lukhele, S. M., Moysi, M., Ogolowa, B. O., Hayes, S. C., Monadjem, A., & Brelsford, A. (2020). VCF data file and code for: CYP2J19 mediates carotenoid colour introgression across a natural avian hybrid zone. *Dryad*. <https://doi.org/10.5061/dryad.jm63xsj87>

Kirschel, A. N. G., Nwankwo, E. C., Seal, N., & Grether, G. F. (2020). Time spent together and time spent apart affect song, feather colour and range overlap in tinkerbirds. *Biological Journal of the Linnean Society*, 129(2), 439– 458. <https://doi.org/10.1093/biolinnean/blz191>

Kurtz, S., Phillippy, A., Delcher, A. L., Smoot, M., Shumway, M., Antonescu, C., & Salzberg, S. L. (2004). Versatile and open software for comparing large genomes. *Genome Biology*, 5(2), R12. <https://doi.org/10.1186/gb-2004-5-2-r12>

LaFountain, A. M., Prum, R. O., & Frank, H. A. (2015). Diversity, physiology, and evolution of avian plumage carotenoids and the role of carotenoid–protein interactions in plumage color appearance. *Archives of Biochemistry and Biophysics*, 572, 201– 212. <https://doi.org/10.1016/j.abb.2015.01.016>

Layard, E. L. (1871). Notes on South-African ornithology. *Ibis*, 13(2), 225– 234. <https://doi.org/10.1111/j.1474-919X.1871.tb05837.x>

Leroi, A. M. (2014). *The lagoon: How Aristotle invented science*. London, UK: Bloomsbury.

Li, H. (2013). Aligning sequence reads, clone sequences and assembly contigs with BWA-MEM. arXiv e-prints, arXiv:1303.3997. <https://ui.adsabs.harvard.edu/abs/2013arXiv1303.3997L>

Li, H., Handsaker, B., Wysoker, A., Fennell, T., Ruan, J., Homer, N., Marth, G., Abecasis, G., & Durbin, R. (2009). The sequence alignment/map format and SAMtools. *Bioinformatics*, 25(16), 2078– 2079. <https://doi.org/10.1093/bioinformatics/btp352>

Lopes, R. J., Johnson, J. D., Toomey, M. B., Ferreira, M. S., Araujo, P. M., Melo-Ferreira, J., Andersson, L., Hill, G. E., Corbo, J. C., & Carneiro, M. (2016). Genetic basis for red coloration in birds. *Current Biology*, 26(11), 1427– 1434. <https://doi.org/10.1016/j.cub.2016.03.076>

Luo, R., Liu, B., Xie, Y., Li, Z., Huang, W., Yuan, J., He, G., Chen, Y., Pan, Q. I., Liu, Y., Tang, J., Wu, G., Zhang, H., Shi, Y., Liu, Y., Yu, C., Wang, B. O., Lu, Y., Han, C., ... Wang, J. (2012). SOAPdenovo2: An empirically improved memory-efficient short-read de novo assembler. *Gigascience*, 1, 2047–217X–1–18. <https://doi.org/10.1186/2047-217x-1-18>

Maia, R., Eliason, C. M., Bitton, P. P., Doucet, S. M., & Shawkey, M. D. (2013). pavo: An R package for the analysis, visualization and organization of spectral data. *Methods in Ecology and Evolution*, 4(10), 906– 913. <https://doi.org/10.1111/2041-210x.12069>

Mayr, E. (1942). *Systematics and the origin of species: From the viewpoint of a zoologist*. New York, NY: Columbia University Press.

McGraw, K. J. (2006). Mechanisms of carotenoid-based coloration. In G. E. Hill & K. J. McGraw (Eds.), *Bird coloration* (Vol. I, pp. 177– 242). Harvard University Press.

Mendes-Pinto, M. M., LaFountain, A. M., Stoddard, M. C., Prum, R. O., Frank, H. A., & Robert, B. (2012). Variation in carotenoid–protein interaction in bird feathers produces novel plumage coloration. *Journal of the Royal Society Interface*, 9(77), 3338– 3350. <https://doi.org/10.1098/rsif.2012.0471>

- Monadjem, A., Passmore, N. I., & Kemp, A. C. (1994). Territorial calls of allopatric and sympatric populations of 2 species of *Pogoniulus* Tinkerbarbet in Southern Africa. *Ostrich*, 65(3–4), 339– 341.
- Mundy, N. I. (2005). A window on the genetics of evolution: MC1R and plumage colouration in birds. *Proceedings of the Royal Society B: Biological Sciences*, 272(1573), 1633– 1640. <https://doi.org/10.1098/rspb.2005.3107>
- Mundy, N. I., Stapley, J., Bennison, C., Tucker, R., Twyman, H., Kim, K.-W., Burke, T., Birkhead, T. R., Andersson, S., & Slate, J. (2016). Red carotenoid coloration in the zebra finch is controlled by a cytochrome P450 gene cluster. *Current Biology*, 26(11), 1435– 1440. <https://doi.org/10.1016/j.cub.2016.04.047>
- Nadeau, N. J., Minvielle, F., Ito, S. I., Inoue-Murayama, M., Gourichon, D., Follett, S. A., Burke, T., & Mundy, N. I. (2008). Characterization of Japanese Quail yellow as a Genomic Deletion Upstream of the Avian Homolog of the Mammalian ASIP (agouti) Gene. *Genetics*, 178(2), 777– 786. <https://doi.org/10.1534/genetics.107.077073>
- Naert, T., Dimitrakopoulou, D., Tulkens, D., Demuynck, S., Carron, M., Noelanders, R., Eeckhout, L., Van Isterdael, G., Deforce, D., Vanhove, C., Van Dorpe, J. O., Creytens, D., & Vleminckx, K. (2020). RBL1 (p107) functions as tumor suppressor in glioblastoma and small-cell pancreatic neuroendocrine carcinoma in *Xenopus tropicalis*. *Oncogene*, 39(13), 2692– 2706. <https://doi.org/10.1038/s41388-020-1173-z>
- Norden, K. K., & Price, T. D. (2018). Historical contingency and developmental constraints in Avian coloration. *Trends in Ecology & Evolution*, 33(8), 574– 576. <https://doi.org/10.1016/j.tree.2018.05.003>
- Nosil, P., & Schluter, D. (2011). The genes underlying the process of speciation. *Trends in Ecology & Evolution*, 26(4), 160– 167. <https://doi.org/10.1016/j.tree.2011.01.001>
- Nwankwo, E. C., Mortega, K. G., Karageorgos, A., Ogolowa, B. O., Papagregoriou, G., Grether, G. F., Monadjem, A., & Kirschel, A. N. G. (2019). Rampant introgressive hybridization in *Pogoniulus* tinkerbirds (Piciformes: Lybiidae) despite millions of years of divergence. *Biological Journal of the Linnean Society*, 127(1), 125– 142. <https://doi.org/10.1093/biolinnean/blz018>
- Nwankwo, E. C., Pallari, C. T., Hadjioannou, L., Ioannou, A., Mulwa, R. K., & Kirschel, A. N. G. (2018). Rapid song divergence leads to discordance between genetic distance and phenotypic characters important in reproductive isolation. *Ecology and Evolution*, 8(1), 716– 731. <https://doi.org/10.1002/ece3.3673>
- Parchman, T. L., Gompert, Z., Mudge, J., Schilkey, F. D., Benkman, C. W., & Buerkle, C. A. (2012). Genome-wide association genetics of an adaptive trait in lodgepole pine. *Molecular Ecology*, 21(12), 2991– 3005. <https://doi.org/10.1111/j.1365-294X.2012.05513.x>

Peterson, B. K., Weber, J. N., Kay, E. H., Fisher, H. S., & Hoekstra, H. E. (2012). Double digest RADseq: An inexpensive method for de novo snp discovery and genotyping in model and non-model species. *PLoS ONE*, 7(5), e37135. <https://doi.org/10.1371/journal.pone.0037135>

Poelstra, J. W., Vijay, N., Bossu, C. M., Lantz, H., Ryll, B., Muller, I., Baglione, V., Unneberg, P., Wikelski, M., Grabherr, M. G., & Wolf, J. B. W. (2014). The genomic landscape underlying phenotypic integrity in the face of gene flow in crows. *Science*, 344(6190), 1410– 1414. <https://doi.org/10.1126/science.1253226>

Raj, A., Stephens, M., & Pritchard, J. K. (2014). fastSTRUCTURE: Variational Inference of Population Structure in Large SNP Data Sets. *Genetics*, 197(2), 573– 589. <http://dx.doi.org.uplib.idm.oclc.org/10.1534/genetics.114.164350>

Saetre, G.-P., Kral, M., & Bures, S. (1997). Differential species recognition abilities of males and females in a flycatcher hybrid zone. *Journal of Avian Biology*, 28(3), 259– 263. <https://doi.org/10.2307/3676978>

Saito, S., & Tasumi, M. (1983). Normal-coordinate analysis of retinal isomers and assignments of Raman and infrared bands. *Journal of Raman Spectroscopy*, 14(4), 236– 245. <https://doi.org/10.1002/jrs.1250140405>

Savitzky, A., & Golay, M. J. E. (1964). Smoothing and differentiation of data by simplified least squares procedures. *Analytical Chemistry*, 36(8), 1627– 1639. <https://doi.org/10.1021/ac60214a047>

Scordato, E. S. C., Wilkins, M. R., Semenov, G., Rubtsov, A. S., Kane, N. C., & Safran, R. J. (2017). Genomic variation across two barn swallow hybrid zones reveals traits associated with divergence in sympatry and allopatry. *Molecular Ecology*, 26(20), 5676– 5691. <https://doi.org/10.1111/mec.14276>

Sommerburg, O., Keunen, J. E. E., Bird, A. C., & van Kuijk, F. J. G. M. (1998). Fruits and vegetables that are sources for lutein and zeaxanthin: The macular pigment in human eyes. *British Journal of Ophthalmology*, 82(8), 907– 910. <https://doi.org/10.1136/bjo.82.8.907>

Stradi, R., Hudon, J., Celentano, G., & Pini, E. (1998). Carotenoids in bird plumage: The complement of yellow and red pigments in true woodpeckers (Picinae). *Comparative Biochemistry and Physiology B-Biochemistry & Molecular Biology*, 120(2), 223– 230. [https://doi.org/10.1016/S0305-0491\(98\)10033-0](https://doi.org/10.1016/S0305-0491(98)10033-0)

Thomas, D. B., & James, H. F. (2016). Nondestructive Raman spectroscopy confirms carotenoid-pigmented plumage in the Pink-headed Duck. *The Auk*, 133(2), 147– 154. <https://doi.org/10.1642/auk-15-152.1>

Thomas, D. B., McGraw, K. J., Butler, M. W., Carrano, M. T., Madden, O., & James, H. F. (2014). Ancient origins and multiple appearances of carotenoid-pigmented feathers in birds.



*Proceedings of the Royal Society B-Biological Sciences*, 281(1788), 20140806.  
<https://doi.org/10.1098/rspb.2014.0806>

Thomas, D. B., McGraw, K. J., James, H. F., & Madden, O. (2014). Non-destructive descriptions of carotenoids in feathers using Raman spectroscopy. *Analytical Methods*, 6(5), 1301– 1308.  
<https://doi.org/10.1039/c3ay41870g>

Toews, D. P. L., Hofmeister, N. R., & Taylor, S. A. (2017). The evolution and genetics of carotenoid processing in animals. *Trends in Genetics*, 33(3), 171– 182.  
<https://doi.org/10.1016/j.tig.2017.01.002>

Toews, D. P. L., Lovette, I. J., Irwin, D. E., & Brelsford, A. (2018). Similar hybrid composition among different age and sex classes in the Myrtle–Audubon's warbler hybrid zone. *The Auk*, 135(4), 1133– 1145. <https://doi.org/10.1642/auk-18-45.1>

Toews, D. P. L., Taylor, S. A., Vallender, R., Brelsford, A., Butcher, B. G., Messer, P. W., & Lovette, I. J. (2016). Plumage genes and little else distinguish the genomes of hybridizing warblers. *Current Biology*, 26(17), 2313– 2318. <https://doi.org/10.1016/j.cub.2016.06.034>

Toomey, M. B., Lopes, R. J., Araújo, P. M., Johnson, J. D., Gazda, M. A., Afonso, S., Mota, P. G., Koch, R. E., Hill, G. E., Corbo, J. C., & Carneiro, M. (2017). High-density lipoprotein receptor SCARB1 is required for carotenoid coloration in birds. *Proceedings of the National Academy of Sciences*, 114(20), 5219– 5224. <https://doi.org/10.1073/pnas.1700751114>

Twyman, H., Andersson, S., & Mundy, N. I. (2018). Evolution of CYP2J19, a gene involved in colour vision and red coloration in birds: Positive selection in the face of conservation and pleiotropy. *BMC Evolutionary Biology*, 18(1), 22. <https://doi.org/10.1186/s12862-018-1136-y>

Twyman, H., Prager, M., Mundy, N. I., & Andersson, S. (2018). Expression of a carotenoid-modifying gene and evolution of red coloration in weaverbirds (Ploceidae). *Molecular Ecology*, 27(2), 449– 458. <https://doi.org/10.1111/mec.14451>

Twyman, H., Valenzuela, N., Literman, R., Andersson, S., & Mundy, N. I. (2016). Seeing red to being red: Conserved genetic mechanism for red cone oil droplets and co-option for red coloration in birds and turtles. *Proceedings of the Royal Society B: Biological Sciences*, 283(1836), 20161208. <https://doi.org/10.1098/rspb.2016.1208>

Veronelli, M., Zerbi, G., & Stradi, R. (1995). In-situ resonance raman-spectra of carotenoids in birds feathers. *Journal of Raman Spectroscopy*, 26(8–9), 683– 692.  
<https://doi.org/10.1002/jrs.1250260815>

Walsh, J., Shriver, W. G., Olsen, B. J., & Kovach, A. I. (2016). Differential introgression and the maintenance of species boundaries in an advanced generation avian hybrid zone. *BMC Evolutionary Biology*, 16(1), 65. <https://doi.org/10.1186/s12862-016-0635-y>

Wang, S., Rohwer, S., de Zwaan, D. R., Toews, D. P. L., Lovette, I. J., Mackenzie, J., & Irwin, D. E. (2019). Selection on a pleiotropic color gene block underpins early differentiation between two warbler species. *bioRxiv*, preprint. <https://doi.org/10.1101/853390>

Weaver, R. J., Santos, E. S. A., Tucker, A. M., Wilson, A. E., & Hill, G. E. (2018). Carotenoid metabolism strengthens the link between feather coloration and individual quality. *Nature Communications*, 9, 73. <https://doi.org/10.1038/s41467-017-02649-z>

Zhang, J. J., Kobert, K., Flouri, T., & Stamatakis, A. (2014). PEAR: A fast and accurate Illumina Paired-End reAd mergeR. *Bioinformatics*, 30(5), 614– 620. <https://doi.org/10.1093/bioinformatics/btt593>

Zhou, X., & Stephens, M. (2012). Genome-wide efficient mixed-model analysis for association studies. *Nature Genetics*, 44(7), 821– 824. <https://doi.org/10.1038/ng.2310>